NOTICE CONCERNING COPYRIGHT RESTRICTIONS

Using QEMSCAN® to Characterize Fracture Mineralization at the Newberry Volcano EGS Project, Oregon: A Pilot Study

Bridget Ayling[1], Peter Rose[1] and Susan Petty[2]

[1]Energy & Geoscience Institute, The University of Utah
[2]AltaRock Energy Inc.

ABSTRACT

We present a pilot study that compares results obtained from QEMSCAN® analyses at the Energy and Geoscience Institute (University of Utah) with other data (petrographic thin section and XRD). Specifically, we present data from representative mineralized fractures intersected in an intermediate-depth (4410 ft) borehole (GEO-N2) at the Newberry Volcano EGS site in Oregon, which is adjacent to the proposed deep (~10 000 ft) EGS well. The Newberry Volcano EGS Demonstration project aims to develop an EGS reservoir in a high-temperature, low-permeability resource on the north-west flank of Newberry Volcano through stimulation of an existing deep well (NWG 55-29) by hydro-shearing techniques. The ability of QEMSCAN® to resolve geochemical zonation in mineralized fractures at a fine resolution ($\geq$ 2 µm scale) and generate quantitative data of the proportion of different secondary minerals in fracture zones is relevant to several aspects of geothermal science and engineering, including assessment of likely effectiveness of chemical and/or hydraulic stimulations, characterizing the relationship between fracture mineralization and rock mechanical properties, and for numerical simulations of water-rock interactions in geothermal systems.

1.0 Introduction

QEMSCAN® (Quantitative Evaluation of Minerals by Scanning Electron Microscopy) is a fully-automated micro-analysis system that enables quantitative chemical analysis of materials and generation of high-resolution mineral maps and images as well as porosity structure (Gottlieb *et al*., 2000). It uses a scanning electron microscopy platform (SEM) with an electron beam source in combination with four energy-dispersive X-ray spectrometers (EDS). The measured backscattered electron and electron-induced secondary X-ray emission spectra are used to classify sample mineralogy. A variety of quantitative information can be obtained including distribution, composition, and angularity of minerals, and the fabric, distribution, texture and porosity of materials.

QEMSCAN® technology was developed in the late 1970's by CSIRO in Australia (the earliest model was called QEM*SEM), and applications were predominately in the minerals industry to complement bulk chemical assay data and to guide decisions in exploration, mining, mineral processing and metal refining (e.g. Miller *et al,* 1982*;* Reid *et al*., 1984). Refinement and modification of the technology has broadened its application to other sectors, including oil and gas (e.g. Edwards and Butcher, 1999; Butcher and Botha, 2010), forensics (Pirrie *et al.,* 2004), planetary geology (e.g. Botha *et al.*, 2008) and general geosciences (e.g. Liu *et al.,* 2005; Grouch *et al*., 2008). Application to geothermal problems has been limited to date (e.g. Hardardottir *et al.*, 2010), but recent improvements in QEMSCAN® software capabilities (refer to Haberleh *et al.,* 2010) that enable customization of raw data interpretation protocols to better suit geothermal mineral assemblages suggest that the potential is immense.

The Newberry Volcano EGS Project is a DoE-funded project operated by AltaRock Energy Inc. The project commenced in 2010, and is forecast to conclude in May 2013. The main objective of the project is to demonstrate the development and operation of an EGS system. The project has several phases including site and resource investigation, stimulation of an existing well to create a geothermal reservoir, production well drilling and completion, testing of well productivity and reservoir characteristics, and conceptual modeling of a commercial-scale EGS well-field and power plant.

For this pilot study, 14 samples of mineralized fractures were collected from core extracted from a shallow (<4500 ft depth) well (GEO-N2) in the Newberry Volcano project area, which is located approximately 1 km from the proposed EGS well (NWG 55-29; ~10 000ft deep). The GEO-N2 samples were collected in the 3400 – 4380 ft depth range. These were then sub-sampled and prepared as polished thin sections. After petrographic observation, seven samples were selected for QEMSCAN® analysis.

2.0 Methods

2.1 QEMSCAN® Analytical Protocols

The analyses were completed at the Energy and Geoscience Institute at the University of Utah, on a QEMSCAN® 4300, which is built on a Zeiss Evo 50 SEM platform with four light element Bruker Xflash energy dispersive X-ray detectors. Energy-dispersive X-ray spectral analysis (EDX) involves the interpretation of secondary X-ray spectra to determine elemental composition, and ultimately mineralogy. The QEMSCAN® system is automated and enables measurement of the EDX spectra along a grid. For information about analytical modes and methodology, refer to Gottlieb *et al*. (2000) and Pirrie *et al*. (2004). This instrument is currently testing beta versions of iMeasure v.5.2 software for the data acquisition, and iDiscover v.5.2 for the spectral interpretation and data processing. The measurements were collected in field-scan mode, and X-ray data were collected every 10µm on the polished thin sections. For this pilot study, total areas measured were ~ 3cm² per sample, which equates to an analysis time of approximately 3 hours. Prior to each analysis, standard instrument tuning was performed, including beam focusing, beam alignment and calibration of the X-Ray detectors and backscatter. A measurement procedure is entered and the analyses are automated. The QEMSCAN® was operated using an accelerating voltage of 20kV and a specimen current of approximately 5 nA.

2.2 QEMSCAN® Classification Protocols

For best results, a suitable classification protocol must be used. A user may use an existing Species Identification Protocol (SIP), modify an existing SIP, or create a new SIP depending on the desired outcome. For example, a SIP developed for measurement of ore deposits and oxides would deliver suboptimal performance when applied to a felsic alumino-silicate rock (e.g. a rhyolite). Mineral definitions included in each SIP can be based on synthetic (i.e. ideal) empirical formulae for mineralogy using the new QEMSCAN® Spectral Analysis Engine (SAE) (which generates synthetic X-ray spectra for a mineral) or, from analysis of standards. Alternatively, examination of a sample under a petrographic microscope for mineral identification followed by analysis by QEMSCAN® enables interactive matching of mineralogy to chemical composition for a sample, and this definition is then the most reasonable for the particular location/project area. XRD or ion-microprobe analyses are also complementary, allowing identification of clay minerals and mineral polymorphs: for this study, five samples were analyzed by XRD for comparison with the QEMSCAN® results, in addition to petrographic observation.

As there is no geothermal-specific SIP that has been developed to date, the SIP used for interpretation of the spectral data in this study was based on a sedimentary SIP, and modified to include geothermal and volcanic-system minerals as needed. Typical geothermal alteration minerals were included in addition to minerals that are known to be present at the Newberry Volcano (as reviewed in Bargar and Keith (1999)). There are two levels at which the user may affect the final mineral classification: first through

the elements that are 'allowed' to be interpreted from the raw X-ray spectra, and secondly through the mineral definitions that are included in SIP. The first stage limits the minerals that can be present: for example, if a Sr-rich calcite is defined in the mineral list, Sr must be present in the element list. It is important to limit the number of elements that can be present to minimize the number of non-unique solutions to the X-ray spectra. Many elemental peaks overlap, and if too many elements are enabled, the number of spurious element results increase (i.e. number of elements for each analysis point) and therefore greater likelihood of not being able to classify each point as a particular mineral because these spurious elements were not included in the mineral definition. For this pilot study, several element lists were trialed, and the final selection included 21 elements.

3.0 Results

The XRD data for the five samples is summarized in Table 1, and the corresponding results from QEMSCAN® for the same samples are summarized in Table 2.

Table 1. XRD results for 5 samples, numbers reflect mass fractions as percentages.

Sample depth in GEO-N2 well (ft)	3469	3763	4263	4341	4348
Smectite	23.5	8			
Illite/smectite			16.4	21.6	28.5
Chlorite/smectite			14.8	20.7	18
Quartz		3.6	27	18.5	16.6
Plagioclase	59.3	66	19.9	19.2	26
K-fledspar	3.3	3			
Clinopyroxene	13.1	16.8			
Calcite			6.2		3.9
Dolomite		0.1	9.7		
Gypsum				17.1	2.9
Anhydrite				1	0.4
Hematite	0.9	2.5	6		3.7
Pyrite				2.1	

Table 2. QEMSCAN® area percentages for the same 5 samples that were analyzed by XRD.

N2-3469	Area %	N2-3763A	Area %	N2-4262B	Area %	N2-4341	Area %	N2-4348	Area %
Plagioclase	54.1	Plagioclase	56.7	Smectites	27	Plagioclase	25.9	Plagioclase	26.5
Smectites	28	Smectites	11.7	Chlorite	19.5	Chlorite	17.4	Smectites	23
Pyroxene	5.1	Pyroxene	7.4	Dolomite	11.3	Smectites	14	Quartz	14.2
Alkali Feldspar	2	Alkali Feldspar	6.1	Quartz	11.1	Sulphate	11.6	Illite	13.1
Iron oxides	1.5	Quartz	3.4	Calcite	10.6	Illite	11.3	Micas	3.1
Micas	1.2	Illite	3.1	Na-Plagioclase	9.8	Quartz	8.5	Calcite	2.6
Olivine	1.1	Olivine	2.4	Garnet	3.4	Micas	2	Zeolites	2.4
Illite	0.5	Oxides	0.8	Iron oxides	1.4	Sulphides	1.1	Chlorite	2
Quartz	0.4	Micas	0.7	Micas	1.3	BaSO4 mud (T)	0.5	Sulphides	2
Garnet	0.2	Iron oxides	0.7	Illite	0.9	Garnet	0.2	Sulphate	1.8
Dolomite	0.2	Apatite	0.4	Olivine	0.1	Apatite	0.2	Iron oxides	0.8
Other	5.4	Amphibole	0.3	Other	3.4	Alkali Feldspar	0.2	Alkali Feldspar	0.6
		Calcite	0.3			Oxides	0.1	Garnet	0.6
		Other	5.6			Other	6.9	Other	6.9

Comparison of the XRD and QEMSCAN® data in Tables 1 and 2 indicates broad agreement between the two techniques. It is reasonable to assume that one will never achieve 100% agreement, reasons being that differences in sampling location may have an effect (i.e. the analyses are collected on adjacent rock surfaces but are still not *exactly* the same piece of material), the QEMSCAN® numbers are for a surface area whereas XRD represents volumetric mass fractions, and also the differences in analytical technique. The QEMSCAN® measures secondary X-rays that are emitted from the sample in response to being hit with an incident electron beam; the secondary X-rays are emitted when electrons jump from a higher-energy shell in an atom to a lower-energy shell, and the number and intensity of the X-rays that are emitted are characteristic for each element. XRD is based on the elastic scattering (diffraction) of X-rays by the electron clouds that surround individual atoms in the sample, and is used to characterize crystallographic structure and mineralogy. XRD is thus able to differentiate mineral polymorphs (e.g. calcite Vs. aragonite) whereas QEMSCAN® cannot. However, XRD is unable to characterize non-crystalline material (amorphous) whereas QEMSCAN® has no problem with this.

For each sample analyzed by QEMSCAN®, there remains a portion of the scan that was not classified (referred to as Other). For these particular samples, this value averages 6%. It does not mean that the elemental composition of these points is unknown, simply that there was no mineral definition in the SIP that was consistent with the measured spectra. Typically these points reflect boundary phases between mineral grains, where the X-Ray spectra generated are composite signals. Alternatively it may represent mineral species that are not defined in the SIP library. This number could be reduced by meticulously defining new 'composite' mineral definitions for the boundary phases present (or new minerals altogether), or alternatively using some of the tools in iDiscover to improve this (e.g. the boundary-phase preprocessor or the measurement de-bugger).

Figures 1 through 5 illustrate the types of data display options and applications that can be accessed via iDiscover. QEMSCAN® enables chemistry and mineralogy to be examined and interpreted in a quantitative manner alongside physical characteristics of the sample such as fracture location, fracture geometry, fracture size, and texture of the rock.

Figure 2. This basaltic andesite sample incorporates a relatively wide fracture zone (10 mm) with extensive secondary mineralization. The different phases of mineral alteration and infilling can be individually observed via tools in the iDiscover software associated with the QEMSCAN® instrument, enabling closer observation of fracture mineral morphology and also potential interpretation of the temporal evolution of fluids passing through the fracture zone.
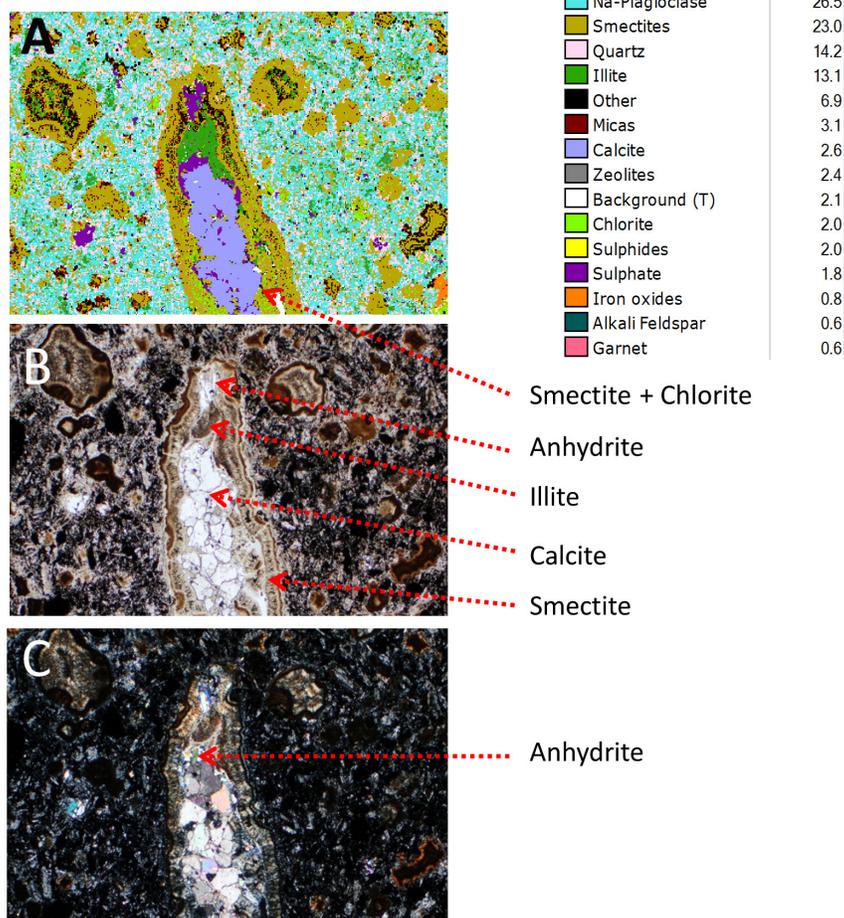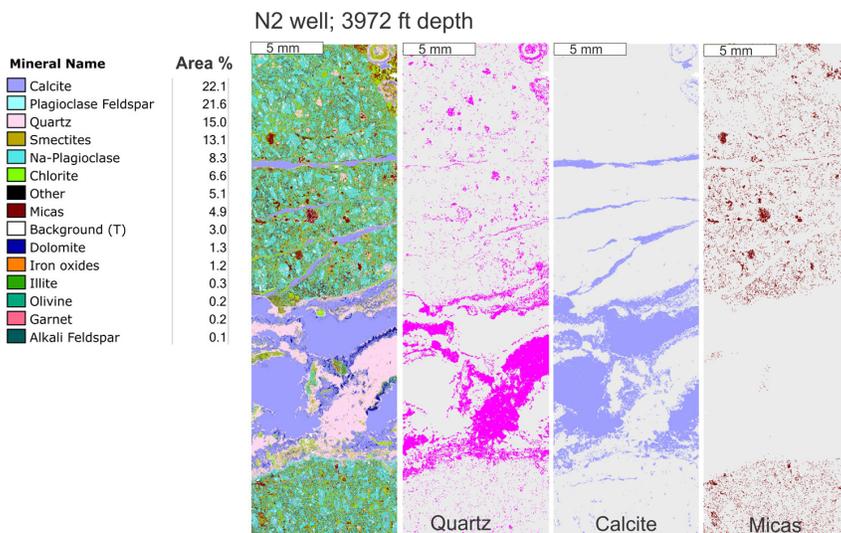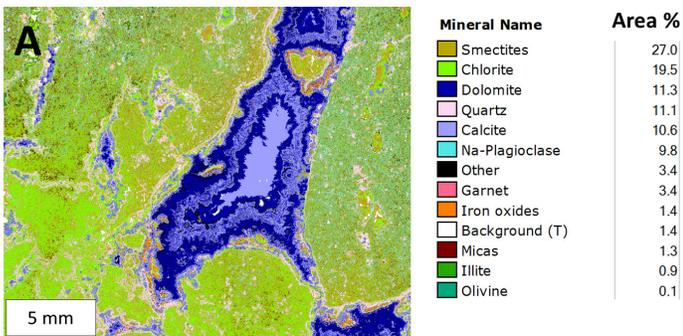

GEO-N2 well: 4348 ft depth

Mineral Name	Area %
Na-Plagioclase	26.5
Smectites	23.0
Quartz	14.2
Illite	13.1
Other	6.9
Micas	3.1
Calcite	2.6
Zeolites	2.4
Background (T)	2.1
Chlorite	2.0
Sulphides	2.0
Sulphate	1.8
Iron oxides	0.8
Alkali Feldspar	0.6
Garnet	0.6

Smectite + Chlorite
Anhydrite
Illite
Calcite
Smectite

Anhydrite

Figure 1. This sample from 4348 ft depth in the GEO-N2 well is a vesicular basaltic andesite, which has undergone pervasive secondary alteration with precipitation of clay minerals, calcite and sulphate minerals. (A) This elongated vesicle is one of many that illustrates multiple stages of secondary cementation. The QEMSCAN® results indicate that smectite clays line most of the vesicles, which are later infilled by either illite, sulphates (anhydrite/gypsum) or calcite. The area percents refer to the whole scan, of which this is a small extract. (B) A photomicrograph of the same vesicle, showing crystallography and the fibrous nature of the smectite clays under plane-polarized light. (C) Cross-polarized image illustrating the calcite and anhydrite cements.

N2 well; 3972 ft depth

Mineral Name	Area %
Calcite	22.1
Plagioclase Feldspar	21.6
Quartz	15.0
Smectites	13.1
Na-Plagioclase	8.3
Chlorite	6.6
Other	5.1
Micas	4.9
Background (T)	3.0
Dolomite	1.3
Iron oxides	1.2
Illite	0.3
Olivine	0.2
Garnet	0.2
Alkali Feldspar	0.1

Quartz   Calcite   Micas

GEO-N2 well: 4262 ft depth

Mineral Name	Area %
Smectites	27.0
Chlorite	19.5
Dolomite	11.3
Quartz	11.1
Calcite	10.6
Na-Plagioclase	9.8
Other	3.4
Garnet	3.4
Iron oxides	1.4
Background (T)	1.4
Micas	1.3
Illite	0.9
Olivine	0.1

GEO-N2 well: 4348 ft depth

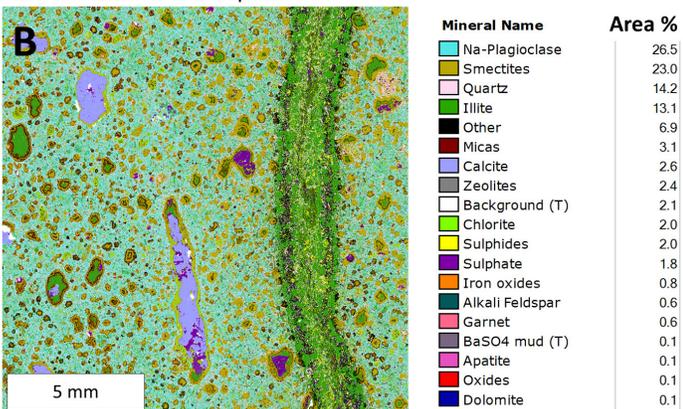| Mineral Name	Area %
Na-Plagioclase	26.5
Smectites	23.0
Quartz	14.2
Illite	13.1
Other	6.9
Micas	3.1
Calcite	2.6
Zeolites	2.4
Background (T)	2.1
Chlorite	2.0
Sulphides	2.0
Sulphate	1.8
Iron oxides	0.8
Alkali Feldspar	0.6
Garnet	0.6
BaSO4 mud (T)	0.1
Apatite	0.1
Oxides	0.1
Dolomite	0.1

Figure 3. (A) QEMSCAN® maps of two samples: the top sample is inferred to represent an altered hydrothermal breccia, with pervasive secondary infilling with calcite and dolomite. Note the oscillatory nature of the calcite and dolomite zones in the large void: perhaps suggestive of different pulses of groundwater recharge to the deeper geothermal system. (B) This vesicular basalt has been altered and little primary porosity remains in the vesicles. These are now infilled with sulphate minerals (anhydrite), calcite, smectite and illite clays. The thin fracture zone appears to be dominated by illite alteration, vs. the matrix material which appears pervasively altered to smectite.
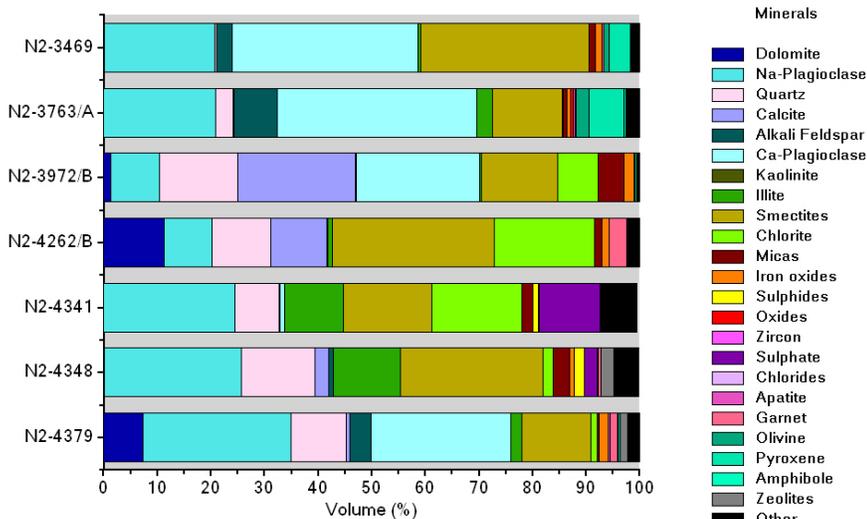

Figure 5. Mineralogy summary for the seven fracture samples collected from the Newberry Volcano GEO-N2 well based on QEMSCAN⁻ analysis (sample includes fractures and surrounding rock; total scan area per sample of ~3cm²). The key alteration minerals that infill the fractures include quartz, calcite/dolomite, sulphates (anhydrite/gypsum), pyrite, illite, chlorite and smectite-group clays.
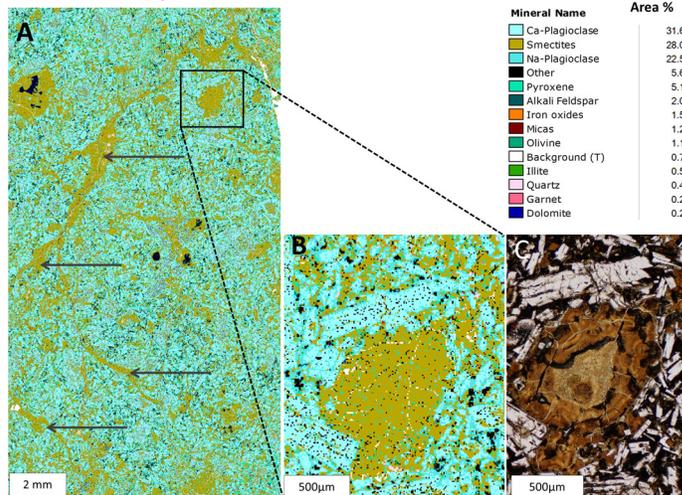
GEO-N2 well: 3469 ft depth

Mineral Name	Area %
Ca-Plagioclase	31.6
Smectites	28.0
Na-Plagioclase	22.5
Other	5.6
Pyroxene	5.1
Alkali Feldspar	2.0
Iron oxides	1.5
Micas	1.2
Olivine	1.1
Background (T)	0.7
Illite	0.5
Quartz	0.4
Garnet	0.2
Dolomite	0.2

Figure 4. Sample N2-3469 is an altered basaltic-andesite: (A) The QEMSCAN® map depicts the clay-filled fractures in the sample (examples are indicated by the arrows) amongst the plagioclase feldspar phenocrysts. Area percent table refers to this map. (B) A zoom in of a smectite-filled feature in the sample. The phenocryst texture is clearly depicted and interstitial clays in between these are clear. (C) Photomicrograph of the same feature as seen under plane polarized light. The fibrous texture of the smectite clays rimming and infilling the feature is distinctive.

4.0 Summary

Automated mineralogy analysis using QEMSCAN® technology is a powerful tool for evaluating spatial distribution of key alteration minerals on the micron-scale and for assessing the relative temporal evolution of fluid chemistries and alteration in a geothermal system. In addition, proportions of these minerals can easily be extracted using the iDiscover software, which has excellent potential for quantifying extensiveness and relative proportions of secondary cements in geothermal fracture systems. QEMSCAN® analyses are complementary to XRD data, benefiting from external validation of major mineral constituents and yet providing significant insight into how these are distributed in the rock. Although there are some differences between the XRD and QEMSCAN® proportions, this pilot study has shown that the results are broadly consistent when the differences in actual sample analyzed and each measurement technique are considered and appreciated.

Acknowledgements

References

Botha, P.W.S.K, Butcher, A.R, Horsch, H.E, Rickman, D, Wentworth, S.J, Schrader, C.M, Stoeser, D, Benedictus, A, Gottlieb, P, and McKay, D. (2008) Ultrafast Phase Mapping of Thin-Sections from An Apollo 16 Drive Tube – a New Visualization of Lunar Regolith. *GSA 2008 Joint Annual Meeting*, 5-9 October 2008, Houston, Texas, Abstract 345-3.

Barger, K.E., and Keith, T.E.C. (1999) Hydrothermal Mineralogy of Core from Geothermal Drill Holes at Newberry Volcano, Oregon. *U.S.G.S. Professional Paper* 1578, 92pp.

Butcher, A.R, and Botha, P.W.S.K. (2010) Automated mineralogy derives key characteristics directly from reservoir rock. *The American Oil & Gas Reporter*, January 2010, 4pp.

Edwards, G.V., and Butcher, A.R. (1999) A new application for QEMSCAN – quantifying the mineralogy of drill cuttings from oil and gas exploration and production wells. *CSIRO Report*, DMR-1140, 97pp.

Goodall, W.R, Scales, P.J, and Butcher, A.R (2005) The use of QEMSCAN and diagnostic leaching in the characterization of visible gold in complex ores. *Minerals Engineering*, Vol. 18(8), pp 877–886.

Gottlieb, P., Wilkie, G., Sutherland, D., Ho-Tun, E., Suthers, S., Perera, K., Jenkins, B., Spencer, S., Butcher, A., Rayner, J., (2000) Using quantitative electron microscopy for process mineralogy applications. *Journal of the Minerals, Metals and Materials Society*, Vol. 52, Number 4, pp 24-25.

Grauch, R.I, Eberl, D.D, Butcher, A.R, and Botha, P.W.S.K (2008) Quantitative mineralogy of fine-grained sedimentary rocks: a preliminary look at QEMSCAN®. *Microscopy and Microanalysis*, Vol. 14(2), pp 532-533.

Haberlah, M., Owen, M., Botha, P.W.S.K., and Gottlieb, P., (2011) SEM-EDS based protocol for subsurface drilling mineral identification and petrological classification. To be presented at the 10th International Congress for Applied Mineralogy (ICAM 2011) in Trondheim, Norway, 1-5 August 2011.

Hardardóttir, V., Hannington, M., Hedenquist, J., Kjarsgaard,I., and Hoal, K. (2010) Cu-Rich Scales in the Reykjanes Geothermal System, Iceland. *Economic Geology,* Vol. 105, pp 1143–1155.

Miller, P.R., Reid, A.F., and Zuiderwyk, M.A. (1982) QEM*SEM image analysis in the determination of modal assays, minerals associations and mineral liberation. *Proceedings of the 14th International Mineral Processing Congress, October 17-23, Toronto, Canada.*

Pirrie, D., Butcher, A.R., Power, M.R., Gottlieb, P., Miller, G.L., (2004) Rapid quantitative mineral and phase analysis using automated scanning electron microscopy (QEMSCAN®); potential applications in forensic geoscience. In: Pye, K., Croft, D.J. (Eds.), Forensic Geoscience, Principles, Techniques and Applications, Vol. 232. *Geological Society Special Publication*, London, pp 23–136.

Reid, A.F., Gottlieb, P., MacDonald, K.J. and Miller, P.J. (1984) QEM*SEM image analysis of ore minerals: volume fraction, liberation and observational variances. *Proceedings of the 2nd International Congress on Applied Mineralogy in the Minerals Industry,* February 22-25, Los Angeles, California.